
Electronic Supplementary Information

Reversible tricolour luminescence switching based on a piezochromic iridium (III) complex

Tianzhi Yang,[a] Yue Wang,[a] Xingman Liu,[a] Guangfu Li,[a] Weilong Che,[a] Dongxia Zhu,*[a] Zhongmin Su*[a] and Martin R. Bryce*[b]

[a] Key Laboratory of Nanobiosensing and Nanobioanalysis at Universities of Jilin Province, Department of Chemistry, Northeast Normal University, 5268 Renmin Street, Changchun, Jilin Province 130024, P.R. China E-mail: zhudx047@nenu.edu.cn, zmsu@nenu.edu.cn

[b] Department of Chemistry, Durham University, Durham, DH1 3LE, UK.

Email: m.r.bryce@durham.ac.uk

Table of Contents

1. Experimental - general information

Materials obtained from commercial suppliers were used without further purification unless otherwise stated. The ligand 2-(1-methyl-1*H*-tetrazol-5-yl)pyridine (Mtzpy) was synthesized by a previously reported procedure.[1] All glassware, syringes, magnetic stirring bars, and needles were thoroughly dried in a convection oven. Reactions were monitored using thin layer chromatography (TLC). Commercial TLC plates were used and the spots were visualized under UV light at 254 and 365 nm. ^{1}H NMR spectra were recorded at 25 °C on a Varian 400 MHz spectrometer with tetramethylsilane (TMS) as internal standard. The chemical shifts (δ) are given in parts per million relative to internal standard TMS (0 ppm). The molecular weight of the complex was obtained by using matrix-assisted laser desorption-ionization time-of-flight (MALDI-TOF) mass spectrometry. Elemental analysis was obtained using a Flash EA1112 analyser. Powder X-ray diffraction (XRD) patterns of the samples were collected on a Rigaku Dmax 2000. TG analyses were performed on a Perkin-Elmer TG-7 analyser heated from room temperature to 800 °C in flowing of nitrogen. Thermal transitions were investigated by a Perkin-Elmer Thermal Analysis DSC-7 under nitrogen at a heating rate 10 °C min^{-1}. Transmission electron microscopy (TEM) images and electron diffraction patterns of the samples were obrained using a TECNAI F20 microscope. The samples were prepared by placing micro-drops of the solution on a holey carbon copper grid. UV-vis absorption spectra were recorded on a Shimadzu UV-3100 spectrophotometer. Photoluminescence spectra were collected on a Shimadzu RF-5301pc spectrophotometer and Maya 2000Pro optical fiber spectrophotometer. PL efficiencies were measured with an integrating sphere (C-701, Labsphere Inc.) with a 365 nm Ocean Optics LLS-LED as the excitation source, and the laser was introduced into the sphere through the optical fiber. The excited-state lifetimes were measured by exciting the samples with 355 nm light pulses with ~3 ns pulse width from a Quanty-Ray DCR-2 pulsed Nd: YAG laser. For the crystal structure of complex **1**, the data were collected on a Bruker Smart Apex II CCD diffractometer.

Toluene and ethanol can slightly dissolve complex **1** and were chosen to facilitate the different crystallization processes. Other solvents, such as dichloromethane, chloroform, acetonitrile, tetrahydrofuran and acetone were also tested. The ground sample was immediately dissolved into a thin film state by these other solvents and the emission colour could not be recovered.

Synthesis and characterization

Synthesis of Mesptz

Benzamide (2.423 g, 20.0 mmol) and *N*,*N*-dimethylformamide dimethyl acetal (2.382 g, 20.0 mmol) were refluxed in toluene (9 mL) for 5 h. After cooling, an off-white solid was precipitated by adding excess petroleum ether to the solution. The intermediate *N*-((dimethylamino)methylene)benzamide was obtained by filtration in a yield of 87%.

A solution of the *N*-((dimethylamino)methylene)benzamide (1.762 g, 10.0 mmol) and 2,4,6-trimethylphenylhydrazine hydrochloride (1.865 g, 10.0 mmol) in 1,4-dioxane (10 mL) and acetic acid (10 mL) was heated to 90 °C for 5 h. Then, the reaction solution was poured into cooled water (100 mL), and neutralized with 2 N NaOH. The mixture was extracted with CH_2Cl_2, and the combined organic phase was dried over anhydrous Na_2SO_4. The solvent was removed under reduced pressure and the residue was purified by column chromatography on silica gel with a mixture of ethyl acetate/petroleum ether (1:8, v/v) as eluent to obtain Mesptz as a white solid (1.363 g, 52%). ^{1}H NMR (400 MHz, $CDCl_3$, ppm): δ 8.16 (s, 1H), 7.51 (dt, J = 7.2, 1.2 Hz, 2H), 7.36 (tt, J = 7.2, 1.6 Hz, 1H), 7.30 (tt, J = 7.6, 1.2 Hz, 2H), 6.98 (s, 2H), 2.36 (s, 3H), 1.91 (s, 6H). Anal. Calcd. for $C_{17}H_{17}N_3$: C 77.52, H 6.46, N 15.96; found: C 77.88, H 7.06, N 15.06.

Synthesis of complex 1

The cyclometalated chloride-bridged dimer [Ir(Mesptz)$_2$Cl]$_2$ was synthesized, according to a procedure described in the literature,[2] by refluxing IrCl$_3$·H$_2$O (0.352 g, 1.0 mmol) with the Mesptz ligand (0.658 g, 2.5 mmol) in the mixture of 2-ethoxythanol (30 mL) and water (10 mL) under a nitrogen atmosphere. A solution of ligand Mtzpy (0.033 g, 0.2 mmol) and the [Ir(Mesptz)$_2$Cl]$_2$ (0.150 g, 0.1 mmol) in dichloromethane (15 mL) and methanol (15 mL) was refluxed for 6 h under a nitrogen atmosphere in the dark. After cooling to room temperature, the mixture was filtered, and then an excess of solid KPF$_6$ was added and stirred for another 0.5 h at room temperature. The solvent was removed under reduced pressure and the residue was purified by silica gel column chromatography using a mixture of ethyl acetate/ dichloromethane (1:10, v/v) as eluent to yield complex **1** (0.147 g, 72%). ^{1}H NMR (400 MHz, CDCl$_3$, ppm): δ 8.68 (d, J = 8.0 Hz, 1H), 8.34 (t, J = 8.0 Hz, 1H), 8.13 (d, J = 6.0 Hz, 1H), 7.73 (s, 1H), 7.58 (t, J = 6.4 Hz, 1H), 7.54 (s, 1H), 7.07 (s, 2H), 7.06 (d, J = 6.4 Hz, 2H), 6.93 (dt, J = 20.0, 7.6 Hz, 2H), 6.76 (dt, J = 25.9, 7.6 Hz, 2H), 6.56 (dd, J = 7.2, 2.4 Hz, 2H), 6.50 (dd, J = 12.4, 7.6 Hz, 2H), 4.74 (s, 3H), 2.41 (d, J = 2.4 Hz, 6H), 2.02 (d, J = 4.1 Hz, 6H), 1.86 (d, J = 21.4 Hz, 6H). MS (MALDI-TOF) [m/z]: 1022.78 (M-PF$_6$). Anal. Calcd. for $C_{41}H_{39}F_6IrN_{11}P$: C 48.09, H 3.81, N 15.05; found: C 48.41, H 3.49, N 15.09.

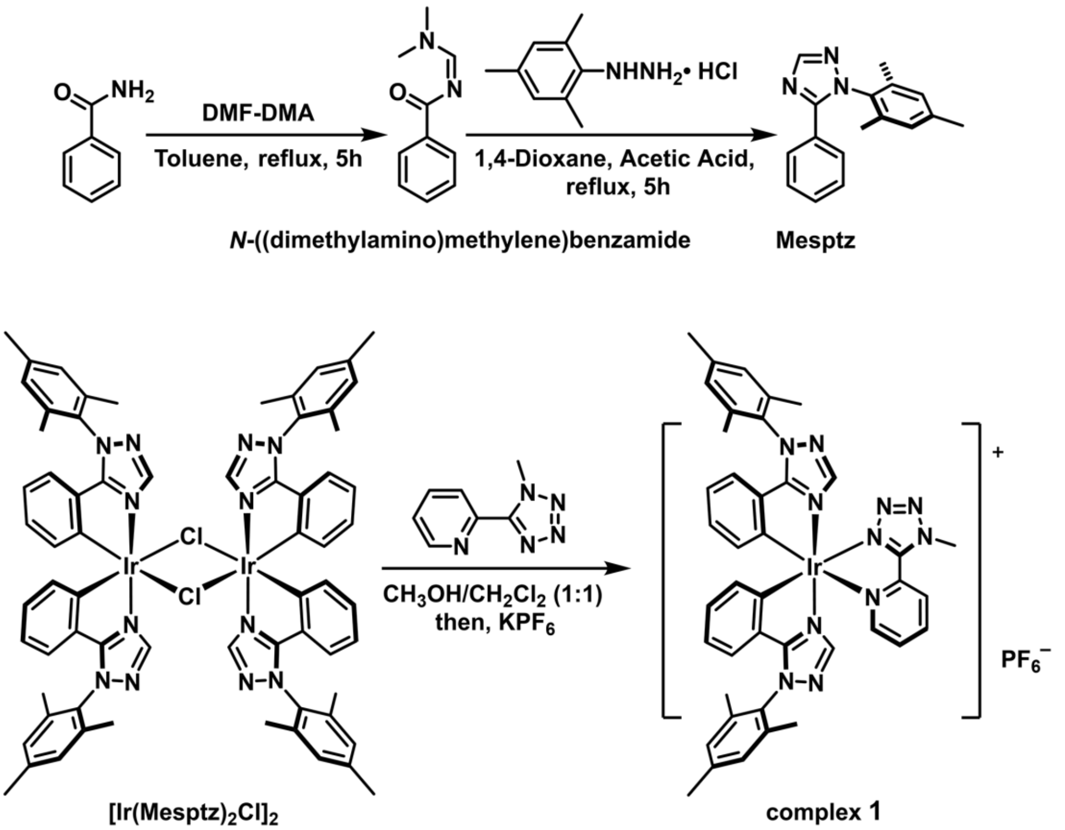

Scheme S1 The synthetic routes to Mesptz and complex **1.**

2. Photophysical properties

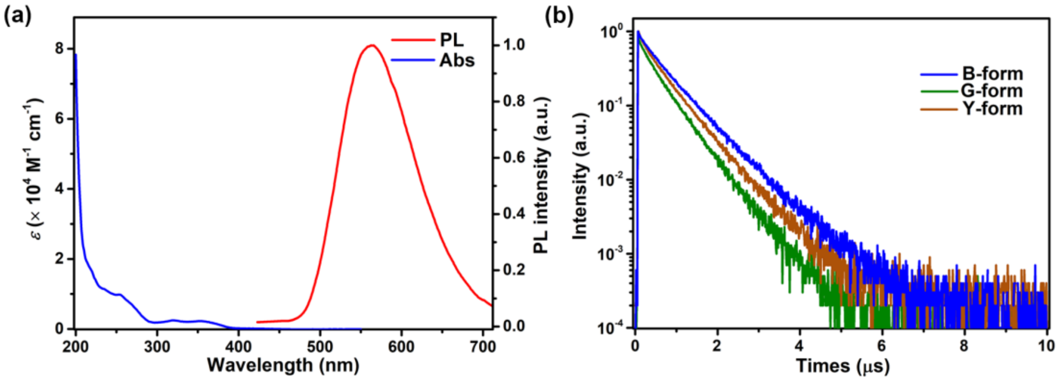

Fig. S1 (a) Absorption and emission spectra of complex **1** in acetonitrile solution. (b) Solid state photoluminescence decay curves of **B**-form, **G**-form and **Y**-form.

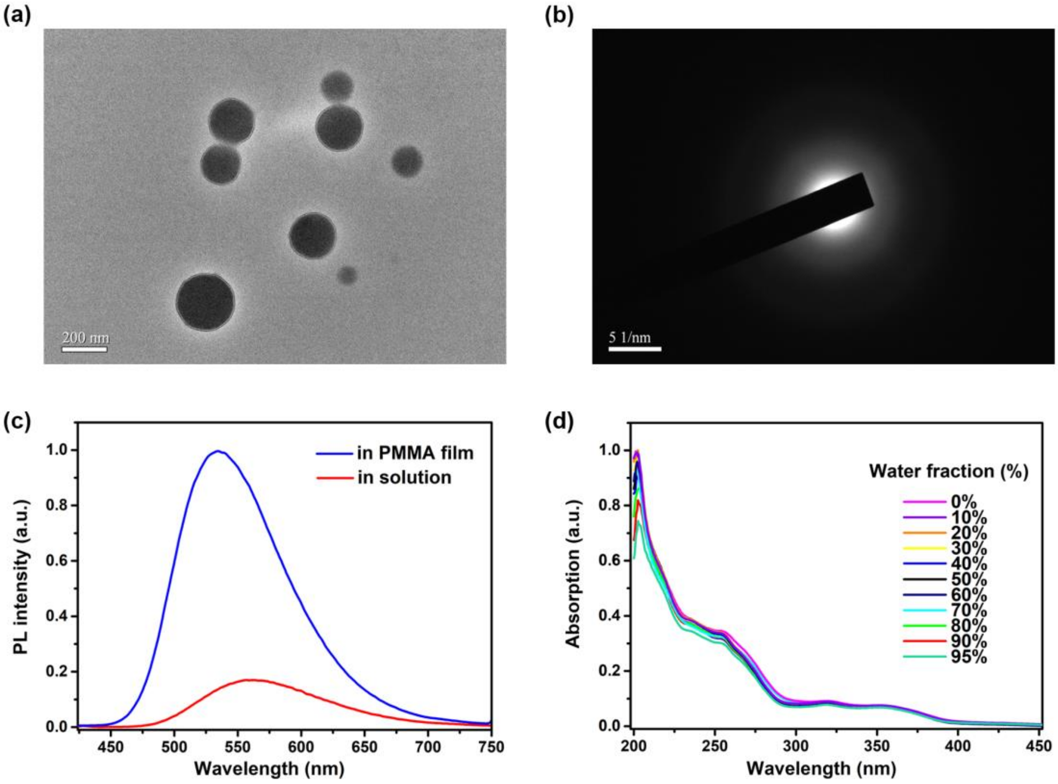

Fig. S2 (a) TEM image of nanoaggregates of complex **1** formed in CH_3CN-H_2O mixture with 95% water fraction. (b) Electron diffraction pattern of the amorphous nanoaggregates. (c) Normalized emission spectra of complex **1** in PMMA film and dichloromethane solution. The doping ratio and solution concentration are both 0.05 wt%. (d) Absorption spectra of complex **1** in CH_3CN-H_2O mixtures with different water fractions.

3. ^{1}H NMR spectra of complex 1 in B-form, G-form and Y-form.

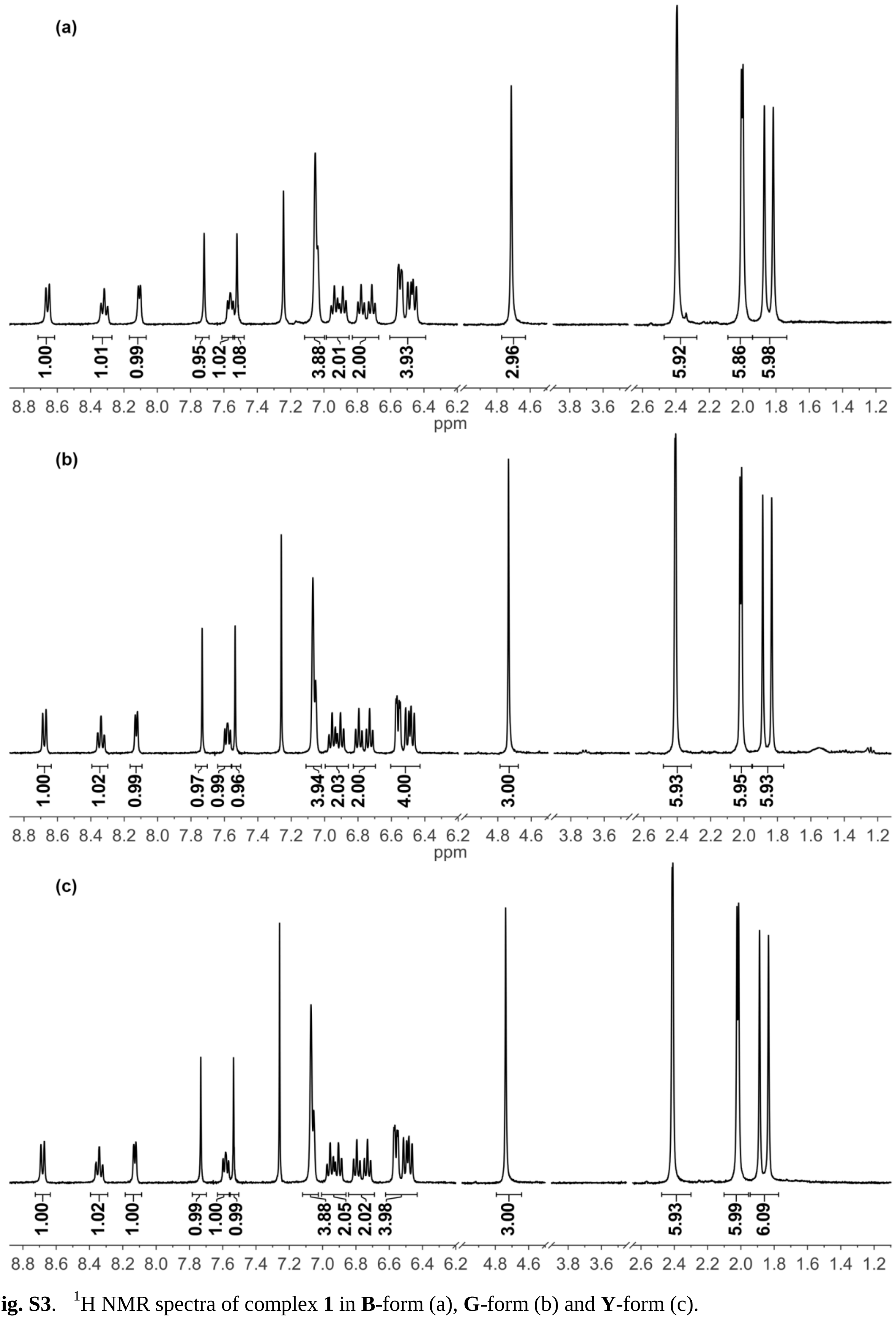

Fig. S3. ^{1}H NMR spectra of complex **1** in **B**-form (a), **G**-form (b) and **Y**-form (c).

4. X-ray crystallographic data

The diffraction data of **B**-crystal was collected on a Bruker Smart Apex II CCD diffractometer with graphite monochromated Cu Kα radiation (λ = 1.54178 Å), while the **G**-crystal data was collected with Mo Kα radiation (λ = 0.71069 Å). Using Olex2, the structure was solved with the SHELXS structure solution program using direct methods and refined with the SHELXL refinement package using least squares minimisation.[3] All non-hydrogen atoms were refined anisotropically, whereas hydrogen atoms were placed at the calculated positions and included in the final stage of refinements with fixed parameters. Crystallographic data for **B**-crystal and **G**-crystal have been deposited with the Cambridge Crystallographic Data Centre with CCDC deposition numbers 1864017 and 1864016. These data can be obtained free of charge from The Cambridge Crystallographic Data Centre via www.ccdc.cam.ac.uk/data_request/cif.

Table S1 Crystal data and structure refinement for **B**-crystal and **G**-crystal.

	B-crystal	**G**-crystal
Empirical formula	$C_{41}H_{39}IrN_{11}\cdot PF_6\cdot 0.5C_7H_8$	$C_{41}H_{39}IrN_{11}\cdot PF_6\cdot C_2H_5OH$
Formula weight	1069.07	1069.07
Temperature (K)	297.14	173
Crystal system	monoclinic	monoclinic
space group	$P2_1/c$	$P2_1/c$
a /Å	20.025(7)	9.025(5)
b /Å	12.326(4)	31.019(5)
c /Å	20.303(6)	15.875(5)
α /°	90	90
β /°	101.211(18)	95.563(5)
γ /°	90	90
V/Å^3	4916(3)	4423(3)
Z	4	4
ρ_{calc}(g/cm^3)	1.445	1.605
μ/mm^{-1}	6.119	3.128
R_{int}	0.0779	0.0508
Goodness-of-fit on F^2	1.068	1.226
$R_1{}^a$, $wR_2{}^b$ [I>2σ(I)]	0.0664, 0.1630	0.0447, 0.0925
R_1, wR_2 (all data)	0.1112, 0.1955	0.0483, 0.0938

[a] $R_1 = \Sigma||Fo| - |Fc||/\Sigma|Fo|$. [b] $wR_2 = \{\Sigma[w(Fo^2 - Fc^2)^2]/\Sigma[w(Fo^2)^2]\}^{1/2}$

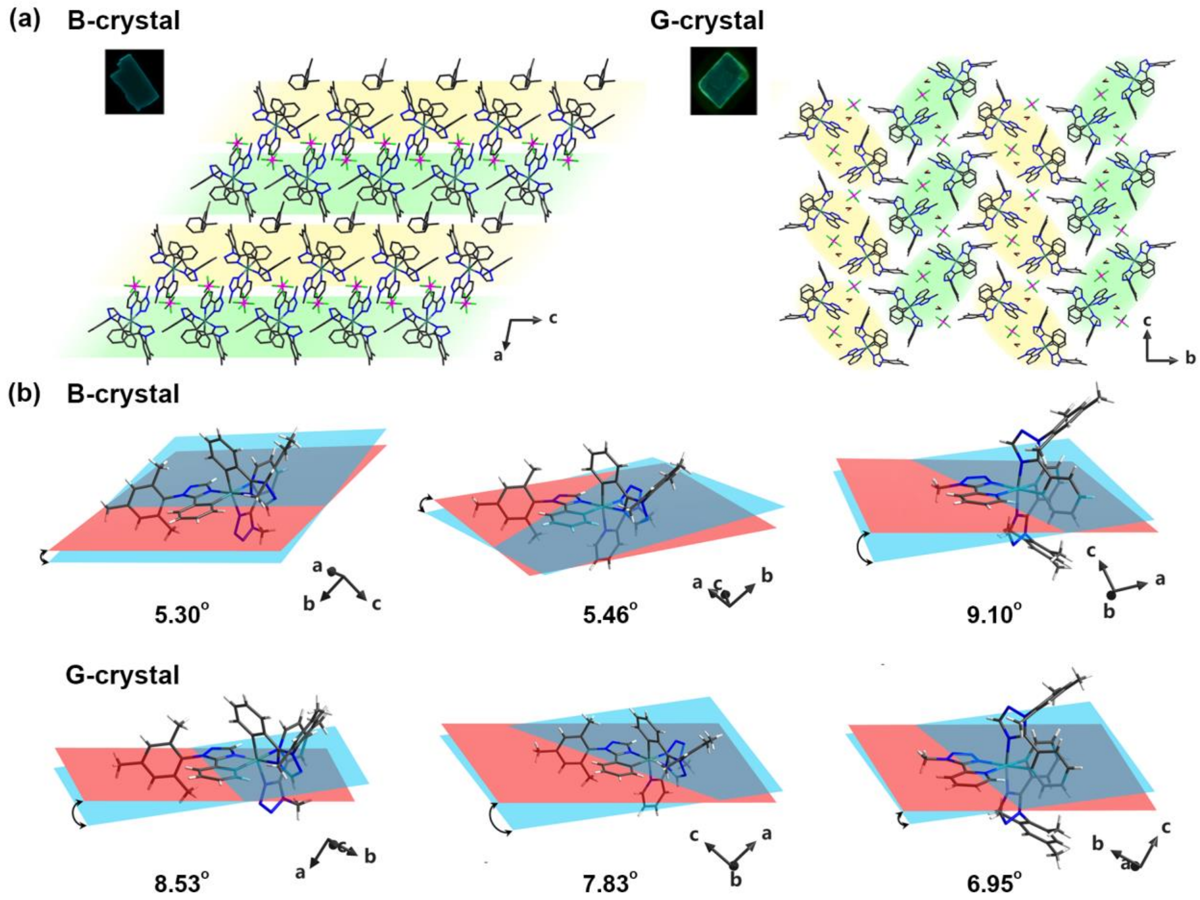

Fig. S4. (a) The molecular arrangements in **B**-crystal and **G**-crystal. (b) The molecular conformational comparison of **B**-crystal and **G**-crystal.

5.Quantum chemical calculations

The ground and excited electronic states of **B**-form and **G**-form were investigated by performing DFT and TD-DFT calculations with the PBE0-1/3 functional. The 6-31G* basis sets were employed for optimizing the C, H, N atoms and the LANL2DZ basis sets for the Ir atom. An effective core potential (ECP) replaces the inner core electrons of iridium leaving the outer core $(5s)^2(5p)^6$ electrons and the $(5d)^6$ valence electrons of Ir(III). All calculations reported here were carried out with the Gaussian 09 software package.[4]

Table S2 The calculated energy levels of the lower-lying transitions of complex **1** in **B**-form and **G**-form.

	States	λ_{cal} (nm)	*f*	Main assignment	Nature
B-form	T_1	496	0	HOMO → LUMO (92.2%)	^{3}MLCT (27.2%)/^{3}LLCT (67.4%)
G-form	T_1	506	0	HOMO → LUMO (87.7%)	^{3}MLCT (24.7%)/^{3}LLCT (70.1%)

6. References

1. G. Li, R. S. Nobuyasu, B. Zhang, Y. Geng, B. Yao, Z. Xie, D. Zhu, G. Shan, W. Che, L. Yan, Z. Su, F. B. Dias and M. R. Bryce, *Chem. - Eur. J.*, 2017, **23**, 11761.
2. S. Sprouse, K. A. King, P. J. Spellane and R. J. Watts, *J. Am. Chem. Soc.*, 1984, **106**, 6647.
3. O. V. Dolomanov, L. J. Bourhis, R. J. Gildea, J. A. K. Howard and H. Puschmann, *J. Appl. Crystallogr.*, 2009, **42**, 339.
4. M. J. Frisch, G. W. Trucks, H. B. Schlegel, G. E. Scuseria, M. A. Robb, J. R. Cheeseman, G. Scalmani, V. Barone, B. Mennucci, G. A. Petersson, H. Nakatsuji, M. Caricato, X. Li, H. P. Hratchian, A. F. Izmaylov, J. Bloino, G. Zheng, J. L. Sonnenberg, M. Hada, M. Ehara, K. Toyota, R. Fukuda, J. Hasegawa, M. Ishida, T. Nakajima, Y. Honda, O. Kitao, H. Nakai, T. Vreven, J. A. Montgomery, Jr., J. E. Peralta, F. Ogliaro, M. Bearpark, J. J. Heyd, E. Brothers, K. N. Kudin, V. N. Staroverov, R. Kobayashi, J. Normand, K. Raghavachari, A. Rendell, J. C. Burant, S. S. Iyengar, J. Tomasi, M. Cossi, N. Rega, J. M. M. Millam, M. Klene, J. E. K. Knox, J. B. C. Cross, V. Bakken, C. Adamo, J. Jaramillo, R. Gomperts, R. E. Stratmann, O. Yazyev, A. J. Austin, R. Cammi, C. Pomelli, J. W. Ochterski, R. L. Martin, K. Morokuma, V. G. Zakrzewski, G. A. Voth, P. Salvador, J. J. Dannenberg, S. Dapprich, A. D. Daniels, O. Farkas, J. B. Foresman, J. V. Ortiz, J. Cioslowski and D. J. Fox, Gaussian 09, Revision A.02, Gaussian, Inc, Wallingford CT, 2009.